THEORETICAL INVESTIGATION OF THE EFFECT OF TEMPERATURE ON THE PHONON DISPERSION RELATION IN GRAPHENE

By

JAFER AHMED UMER

A PROJECT SUBMITTED TO THE GRADUATE PROGRAM STUDIES OF THE ADDIS ABABA UNIVERSITY IN PARTIAL FULFILLMENT OF THE REQUIREMENTS FOR THE DEGREE OF MASTER OF SCIENCE IN PHYSICS (CONDENSED MATTER)

ADDIS ABABA UNIVERSITY

COLLEGE OF NATURAL AND COMPUTATIONAL SCIENCE

DEPARTMENT OF PHYSICS

March 2021

Addis Ababa, Ethiopia

ADDIS ABABA UNIVERSITY

PROGRAM OF GRADUATE STUDIES

DEPARTMENT OF PHYSICS

THEORETICAL INVESTIGATION OF THE EFFECT OF TEMPERATURE ON THE PHONON DISPERSION RELATION IN GRAPHENE.

A PROJECT SUBMITTED TO THE GRADUATE PROGRAM STUDIES OF THE ADDIS ABABA UNIVERSITY IN PARTIAL FULFILLMENT OF THE REQUIREMENTS FOR THE DEGREE OF MASTER OF SCIENCE IN PHYSICS (CONDENSED MATTER)

Jafer Ahmed

	Signature	Date
Examiners		
1. Dr. Cherinet Amente	_____	_____
2. Dr. Belayneh Mesfin	_____	_____
Advisors: - Dr. Tesgera Bedassa	_____	_____

Addis Ababa, Ethiopia

Abstract

We have reviewed the temperature dependence of the phonon dispersion relation in graphene [1]. The dispersion relation of graphene was calculated in the harmonic approximation with an empirical potential of long-range carbon bond order potential (LCBOP) [2]. Then, some thermodynamic quantities in the quasiharmonic approximation were calculated, using the same potential. By using LCBOP then calculated the temperature dependence of the phonon dispersion relation and of the bending rigidity in graphene. And also we can summarize that the temperature dependence of the bending rigidity is due to combining in the whole phonon spectrum and calculation of this dependence was not in spite of that possible, since we reviewed possible strategies to adapt the method to this situation.

Acknowledgements

First of all, I would like to thanks to the Almighty Allah for helping me throughout this paper and my life.

I would like to thank my project advisor Dr. Tesgera Bedassa for his whole hearted professional advice and guidance by giving constructive comments and useful suggestions.

I am grateful to my wife for her great love and supports without complain of regret has enabled me to complete this MSc project. I have to express my sincere; genuine and honest appreciation to my family they form the backbone and origin of my happiness.

Special thanks are also give to my group mates .Their encouragement and always supportive throughout this work. It is not sufficient to express my gratitude with only a few words.

Finally I would like to dedicate this paper for the memory of Moneti Jafer my child.

Table of Contents

Lists of figures

INTRODUCTION

Graphene is a recently discovered and very promising crystal. Graphene is a two-dimensional structure consisting of carbon atoms closely packed in a honeycomb lattice and the phonon dispersion relation in graphene in the harmonic approximation with an empirical potential LCBOP developed and calculated by J.H. Los and A. Fasolino [3]. The material is recently discovered and a lot of fundamental research can still be done to unveil its properties and the physics behind it.

This project is incorporated as a continuation and extension of the work done by Leendertjan Karssemeijer [4]. He calculated, among other things, for two-dimensional materials it is known that the acoustic out-of-plane mode has a quadratic dispersion, as shown by Lifshitz [5]. Since the mode is quadratic, it has low frequencies for a large range of wave vectors. This means that this mode is easily populated even for low temperatures. Therefore, L. Karssemeijer and A. Fasolino tried to include some an harmonic effect by using the quasiharmonic approximation. The quasiharmonic approximation reproduced the negative thermal expansion coefficient of graphene. At high enough temperatures, the lattice parameter that minimises the quasiharmonic free energy becomes quite small and the material becomes dynamically unstable, namely imaginary frequencies occur in the harmonic approximation. The aim of this project is to include anharmonic effects in the calculation of the phonon dispersion relation by different method developed by P. Souvatzis et al. [6]. To understand this method and to interpret the results, it is important to understand the harmonic approximation and the quasiharmonic approximation. Therefore, this project begins with the harmonic and quasiharmonic approximations and ordered in the following way:

The first chapter introduces some general properties of graphene as a crystal and the second contains the theory of lattice dynamics in the harmonic approximation. Chapter 3 introduces the empirical potential LCBOP and electrical potential that we used for all our calculations. Chapter 4 describes how we calculated the phonon dispersion relation in the harmonic approximation and with the quasiharmonic approximation some thermodynamic quantities are calculated. This chapter will give results for the thermal expansion coefficient of graphene, calculated in two different ways.

1. GRAPHENE

This chapter introduces the crystal structure of graphene in real space and in reciprocal space. In reciprocal space, we give the points and a line with high symmetry, since paths along these lines is frequently used to display the phonon dispersion relation.

1.1. Crystal Structure and overview properties

Graphene is a 2-dimensional crystal structure in which the carbon atoms are arranged in a honeycomb lattice (see figure 1.1). The 2D carbon system graphene thus forms a honeycomb lattice. The atoms are separated by a distance $a \approx 1.42$Å. The honeycomb lattice is not a Bravais lattice but is built up from two triangular sublattices (A & B) with separation of

$$\delta = \begin{pmatrix} 1 \\ 0 \end{pmatrix}.$$

These are shown in figure 1.1 as two filled circles. Graphene thus has a triangular lattice with two atoms per unit cell. The unit cell has the following lattice vectors:

$$\vec{a}_1 = a\begin{pmatrix} \sqrt{3} \\ 0 \end{pmatrix}, \qquad \vec{a}_2 = \frac{1}{2}a\begin{pmatrix} \sqrt{3} \\ 3 \end{pmatrix} \tag{1.1}$$

where a is the length of the basis vectors and $a = \sqrt{3}a_{cc}$, where a_{cc} is the distance between the nearest neighbours.

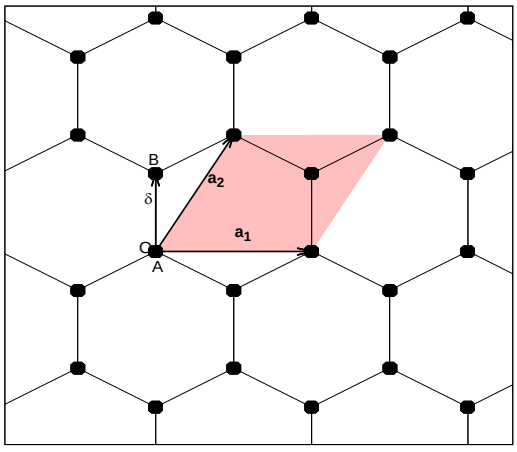

Figure 1.1: Graphene lattice [6]

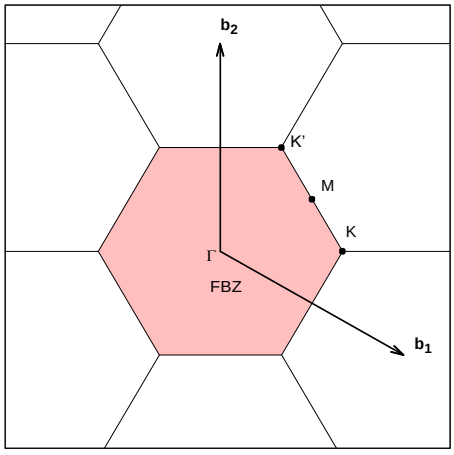

Figure 1.2: Brillouin zone [6]

1.2. Reciprocal Space

In physics, the reciprocal lattice represents the Fourier transform of another lattice (usually a Bravais lattice). In normal usage, the initial lattice (whose transform is

represented by the reciprocal lattice) is usually a periodic spatial function in real-space and is known as the *direct lattice*. While the direct lattice exists in real-space and is what one would commonly understand as a physical lattice, the reciprocal lattice exists in reciprocal space (also known as *momentum space* or less commonly known as *K-space*, due to the relationship between the momentum and position).

The reciprocal of a reciprocal lattice is the original direct lattice, since the two are Fourier transforms of each other.

For most of the calculations in solid state physics we use the reciprocal lattice of a crystal. If the real space is $\vec{R} = n_1\vec{a}_1 + n_2\vec{a}_2 + n_3\vec{a}_3 \;\; n_i \in \{0, \pm1, \pm2, \pm3, \dots\}$ this is real space we define the vectors of the reciprocal lattice, G by $e^{i\vec{G}\,\vec{R}} = 1$.

Then we can construct primitive lattice vectors of the reciprocal lattice vectors are with the following identity:

$$\vec{a}_i \cdot \vec{b}_j = 2\pi\delta_{ij} \qquad \text{where } \delta_{ij} = \begin{cases} 1 \; if \; i = j \\ 0 \; if \; i \neq j \end{cases}.$$

This can be satisfied in three dimensions if,

$$\vec{b}_1 = \frac{2\pi\,\vec{a}_2 \times \vec{a}_3}{\vec{a}_1 . \vec{a}_2 \times \vec{a}_3}, \qquad \vec{b}_2 = \frac{2\pi\,\vec{a}_3 \times \vec{a}_1}{\vec{a}_1 . \vec{a}_2 \times \vec{a}_3}, \qquad \vec{b}_3 = \frac{2\pi\,\vec{a}_1 \times \vec{a}_2}{\vec{a}_1 . \vec{a}_2 \times \vec{a}_3}.$$

This gives the following reciprocal lattice vectors for graphene:

$$\vec{b}_1 = \frac{2\pi}{a}\begin{pmatrix} 1 \\ -\frac{1}{\sqrt{3}} \end{pmatrix} \qquad \vec{b}_2 = \frac{2\pi}{a}\begin{pmatrix} 0 \\ \frac{2}{\sqrt{3}} \end{pmatrix} \tag{1.2}$$

Then we can write $\vec{G} = m_1\vec{b}_1 + m_2\vec{b}_2 + m_3\vec{b}_3$, $m_i \in \{0, \pm1, \pm 2, \pm3, \}$. This is reciprocal spaces.

By connecting real and reciprocal spaces, we note that

$$e^{i\vec{G}\cdot\vec{R}} = e^{i2\pi(m_1n_1 + m_2n_2 + m_3n_3)} = 1$$

which, if n_i are integer is equal to 1, if and only if m_i is also integer.

The scalar product between a vector in the direct and a vector in the reciprocal lattice is expressed simply in terms of their components in direct and reciprocal lattice basis vectors.

$$\text{If} \quad \vec{r} = \vec{r}_1 a_1 + \vec{r}_2 a_2 + \vec{r}_3 a_3 \qquad (i)$$

and

$$\vec{q} = \vec{q}_1 b_1 + \vec{q}_2 b_2 + \vec{q}_3 b_3 \qquad (ii)$$

then using the scalar product the equation becomes to

$$\vec{r} \cdot \vec{q} = \vec{r}_1 \vec{q}_1 + \vec{r}_2 \vec{q}_2 + \vec{r}_3 \vec{q}_3$$

with these reciprocal vectors, one can construct the first Brillouin zone, which is shown in figure 1.2. In this figure, some points with special symmetry (***Γ, K, K′***, and ***M***) are denoted. The coordinates of these special points in reciprocal space are:

$$\boldsymbol{\Gamma} = \frac{2\pi}{a}\begin{pmatrix}0\\0\end{pmatrix},\ \boldsymbol{K} = \frac{2\pi}{a}\begin{pmatrix}\frac{2}{3}\\0\end{pmatrix},\ \boldsymbol{K'} = \frac{2\pi}{a}\begin{pmatrix}\frac{1}{3}\\\frac{1}{\sqrt{3}}\end{pmatrix},\ \boldsymbol{M} = \frac{2\pi}{a}\begin{pmatrix}\frac{1}{2}\\\frac{1}{2\sqrt{3}}\end{pmatrix}.$$

These points are highly symmetrical and the lines among them have special symmetry. Phonon dispersion relations are often calculated and displayed along the lines that connect these points.

1.3. Graphene applications

Graphene has strongly attracted scientific and technological interest. It has shown great promise in many applications, such as field effect transistors, electrochemical sensors and biosensors, transparent conductive films, graphene-polymer nano composites, energy storage and conversion units, and solar cells [58, 68, 69].

Graphene can be used for the following applications.

- Electronics

  → Sensors, transistors, interconnects, printable electronics

- Transparent displays.

- Power storage

  → Battery, electrodes, super−capacitors

- Medicine

  ⟶ Membranes, sensors

2. LATTICE DYNAMICS

In a crystal all atoms have a certain equilibrium position. Together, these positions form the crystal lattice. In crystals at finite temperatures, the atoms are not exactly at their ideal position: they oscillate around this position. One could describe these oscillations atom by atom; but this would be very cumbersome for large systems. There is a very powerful theorem for infinite systems, the Bloch theorem, which allows us to describe these oscillations as Collective waves. These waves can be seeing as a kind of particles (quasiparticles) is called phonons. These quasiparticles have a certain dispersion relation depending on the material: the phonon dispersion relation. In this project, we will focus on the review of temperature dependence of the phonon dispersion relation in graphene. Before discussing temperature, in this chapter the harmonic theory of lattice dynamics will be explained. In the end of the chapter, we will look at some symmetry properties for graphene. Moreover we will explain how one can obtain the bending rigidity for two – dimensional materials from the phonon dispersion relation.

2.1 Theory of lattice dynamics

Consider an infinite layer of graphene. The atoms have a minimum energy position in relation to the other atoms. We allow the atoms to vibrate around these minima. Describing these vibrations results in the quasi-particle description of phonons. Here we present some of the basics of the theory of lattice dynamics and explain how the phonon spectra can be calculated.

In a crystal we can identify a unit cell that is periodically repeated to represent the infinite sample. The basis vectors the unit cell are a_1, a_2 and a_3. All lattice points are located at integer combinations of these vectors. We can therefore introduce the vector $R_l = l_1 a_1 + l_2 a_2 + l_3 a_3$.

Every unit cell contains N atoms labeled by k, the vector d_k gives all atomic positions within the unit cell. An example is given in figure 1.1. If we denote the displacements of the atoms with the vector $u_{l.k}$ we can write all atom coordinates as $r_{l,k} = R_l + d_k + u_{l.k}$.

We can expand the potential $V(r_{l,k})$ around the equilibrium positions

$$V\left(r_{\mathrm{l},k}^{\alpha}\right) = V_0 + \sum_{\mathrm{l},k,\alpha}\left[\frac{\partial V}{u_{\mathrm{l},k}^{\alpha}}\right]u_{\mathrm{l},k}^{\alpha} + \frac{1}{2}\sum_{\mathrm{l},k,\alpha}\sum_{\mathrm{l}',k',\beta}\left[\frac{\partial^2 V}{u_{\mathrm{l},k}^{\alpha}u_{\mathrm{l}',k'}^{\beta}}\right]u_{\mathrm{l},k}^{\alpha}u_{\mathrm{l}',k'}^{\beta} + \cdots \qquad (2.1)$$

where the three Cartesian coordinates are indicated by the Greek indices. The leading term at the right-hand side V_0 gives the total potential energy when the atoms are in the equilibrium position and is a constant. Furthermore, since the potential at the equilibrium position is minimal, the second term on the right-hand side vanishes. All the interesting physical phenomena come from the quadratic and higher order terms. Truncating (cutting off) the expansion at the second order results in the *harmonic approximation*. It is a valid assumption when the displacements are small.

The Hamiltonian of the system contains, in the harmonic approximation, a term for the cohesive energy of the equilibrium configuration (the constant V_0), the kinetic energy of the atoms and the quadratic term of equation 2.1. The equation of motion then becomes

$$M_k\ddot{u}_{l,k}^{\alpha} = \frac{\partial V}{\partial u_{\mathrm{l},k}^{\alpha}} = -\sum_{l',k',\beta}\phi_{l,k;l'k'}^{\alpha,\beta}u_{l',k'}^{\beta} \qquad (2.2)$$

where we have introduced the mass M_k and the force constants ϕ:

$$\phi_{l,k;l'k'}^{\alpha,\beta} = \left[\frac{\partial^2 V}{u_{\mathrm{l},k}^{\alpha}u_{\mathrm{l}',k'}^{\beta}}\right]_0 . \qquad (2.3)$$

The force constants matrix gives us the force exerted on atom (l,k) in the α direction by the atom (l',k') when the latter is displaced in the β direction while all other atoms are kept in their equilibrium position [26].

The definition in equation 2.3 satisfies the condition

$$\phi_{l,k;l'k'}^{\alpha,\beta} = \phi_{l'k';l,k}^{\beta,\alpha} \qquad (2.4)$$

since the order of partial derivatives is arbitrary. Besides this symmetry, the forces must not change when the whole sample is rigidly displaced by any vector v. This means that when substituting $u_{\mathrm{l}',k'}^{\beta}$ by $u_{\mathrm{l}',k'}^{\beta} + v^{\beta}$, the result must be the same. Using this requirement of translational invariance in equation 2.2 directly implies:

$$\sum_{l',k',\beta} \phi^{\alpha,\beta}_{l,k;l'k'} = 0. \tag{2.5}$$

We can also displace the lattice through a lattice translation vector $\mathrm{X_l}$ i.e. $\mathbf{R}_{\mathrm{l},k} \rightarrow \mathbf{R}_{\mathrm{l},k} + \mathrm{X}_m$. But since it is a lattice vector we can write:

$$\mathbf{R}_{\mathrm{l},k} + \mathrm{X_m} = \mathbf{R}_{\mathrm{l+m},k}. \tag{2.6}$$

Furthermore, the interatomic forces will not change so $\phi^{\alpha,\beta}_{\mathrm{l+m},k;\mathrm{l}'+\mathrm{m},k'} = \phi^{\alpha,\beta}_{l,k;l'k'}$. Choosing m = $-l$ or $-\,l'$ we get

$$\phi^{\alpha,\beta}_{l,k;l'k'} = \phi^{\alpha,\beta}_{0,k;l'-l,k'} = \phi^{\alpha,\beta}_{\boldsymbol{l'-l},k;0,k'} \tag{2.7}$$

and we see that the dependence of the forces on l and l' works only via their difference. We will use these symmetry properties of ϕ later on.

Because the lattice is periodic for translations of a lattice vector we expect the solutions to equation 2.2 to share this property. We therefore consider solutions of the form of

$$u^{\alpha}_{\mathrm{l},k} = \frac{u^{\alpha}_{k}(q)}{\sqrt{M_k}}\, e^{i(q.R_l - \omega t)} \tag{2.8}$$

i.e. a plane wave solution with frequency ω, wavevector q and amplitude $u^{\alpha}_{k}(q)$. By substituting equation 2.8 into the equation of motion we end up with

$$\omega^2 u^{\alpha}_{k}(q) = \sum_{k',\beta} D^{\alpha,\beta}(k,k',q) u^{\beta}_{k'}(q) \tag{2.9}$$

where we have defined the *dynamical matrix* :

$$D^{\alpha,\beta}((k,k',q) = \frac{1}{\sqrt{M_k M'_k}} \sum_{l'} \phi^{\alpha,\beta}_{l,k;l'k'}\, e^{iq.\left(\boldsymbol{R}_{\mathrm{l}'} - \boldsymbol{R}_{\mathrm{l}}\right)}. \tag{2.10}$$

It can be easily shown that the dynamical matrix is Hermitian:

$$\left[D^{\alpha,\beta}((k,k',q)\right]^{*} = \frac{1}{\sqrt{M_k M'_k}} \sum_{l'} \phi^{\alpha,\beta}_{l,k;l'k'}\, e^{-iq.\left(\boldsymbol{R}_{\mathrm{l}'} - \boldsymbol{R}_{\mathrm{l}}\right)}$$

$$= \frac{1}{\sqrt{M_k M'_k}} \sum_{l'} \phi^{\beta,\alpha}_{l'k';l,k}\, e^{-iq.\left(\boldsymbol{R}_{\mathrm{l}'} - \boldsymbol{R}_{\mathrm{l}}\right)}$$

$$= \frac{1}{\sqrt{M_k M'_k}} \sum_{l'} \phi^{\beta,\alpha}_{2l-l'k';l,k}\, e^{-iq.\left(\boldsymbol{R}_{\boldsymbol{2l-\mathrm{l}'}} - \boldsymbol{R}_{\mathrm{l}}\right)}$$

$$= \frac{1}{\sqrt{M_k M'_k}} \sum_{l'} \phi^{\beta,\alpha}_{l,k';l',k} \; e^{-iq.\left(\boldsymbol{R}_l - \boldsymbol{R}_{l'}\right)}$$

$$\left[D^{\alpha,\beta}((k,k',q)\right]^* = D^{\beta,\alpha}(k',k,q). \tag{2.11}$$

Equation 2.9 is a set of 3N coupled linear differential equations yielding the amplitudes of the displacements at each frequency. The frequency spectrum is given by the eigenvalue equation

$$\left|D^{\alpha,\beta}((k,k',q) - \omega^2(q)\delta_{\alpha,\beta}\delta_{k,k'}\right| = 0 \tag{2.12}$$

Since the dynamical matrix is Hermitian, for each value of q there are 3N real solutions for $\omega^2(q)$. This means that $\omega(q)$ is real or purely imaginary. Because the amplitudes of the displacements in equation (2.8) grow exponentially for imaginary frequencies, the lattice is not stable if these solutions occur. This could happen when the studied sample was not in the minimum energy configuration of the potential.

2.2. Properties for Graphene

2.2.1. Symmetry Properties

From the symmetry properties of the graphene crystal, we can deduce certain features of the phonon dispersion relation. The mirror symmetry in the graphene plane implies:

$$\phi_{xz}(lk, l'k') = \phi_{yz}(lk, l'k') = 0$$

This means that the out – of – plane modes are separate from the in – plane modes in this approximation. Taking into account that the two sub lattices of graphene as shown in figure 1.1 are equivalent, we see that the two parts of the dynamical matrix belonging to each of the two should be the same:

$$D^{\alpha,\beta}(1,1,q) = D^{\alpha,\beta}(2,2,q)$$

From the condition for translational invariance (eq. (2.4)) and the definition of the dynamical matrix (eq. (2.9)) we can see that at the zone centre ($q = 0$):

$$D^{\alpha,\beta}(1,1,q=0) + D^{\alpha,\beta}(1,2,q=0) = 0$$

These considerations lead to six phonon branches from which two are purely out – of – plane and four are in – plane modes. The three acoustical modes are for small q translational modes. The optical modes at q= *zero* are modes where the atoms move

in the unit cell and the centre of mass of the unit cell does not move.

The acoustic out – of – plane mode is taking by:

$$\omega_{ZA}^2(q) = D_{zz}(1,1,q) + D_{zz}(1,2,q). \tag{2.17}$$

The optical out – of – plane mode is set by

$$\omega_{ZO}^2(q) = D_{zz}(1,1,q) - D_{zz}(1,2,q).$$

The two acoustical in – plane modes are given by the eigenvalues of:

$$D^{\alpha,\beta}(1,1,q) + D^{\alpha,\beta}(1,2,q). \qquad \alpha,\beta = x,y$$

The two optical in – plane modes are given by the eigenvalues of

$$D^{\alpha,\beta}(1,1,q) - D^{\alpha,\beta}(1,2,q) \qquad \alpha,\beta = x,y.$$

2.2.2. Bending Rigidity

In this project, we will focus on the flexural phonons. These are the phonons of the acoustic out – of – plane mode. Waves propagating in thin plates, membranes or two – dimensional crystals are fundamentally different from waves in three – dimensional materials. The dispersion of the longitudinal waves in particular shows a strange type of behavior: it is quadratic in the wave vector near the zone center. This paragraph contains two ways to calculate the dispersion of the out – of – plane waves near the zone center. The first way uses the argument of rotational invariance, which imposes a condition on the force constants that leads to a condition on the eigenvalues of the dynamical matrix. The second way is by means of the theory of elasticity. An equation of equilibrium is derives from the minimum of the free energy. This gives an equation of motion, which gives the dispersion relation near the zone center. We give the dispersion relation for the acoustic out – of – plane phonon mode in the most general form at the end of this paragraph.

i. Rotational Invariance

Analogously (comparable) to the condition of translational invariance in three – dimensional materials (eq. (2.5)), we can define a condition of rotational invariance for two – dimensional materials in three – dimensional space. The lattice could be rotated by a uniform in – plane rotation. The rotation may not cause any forces or torques. This condition of rotational invariance implies

$$\sum_{l'k'} \phi_{ZZ}(lk, l'k') R_{l'}^{\alpha} R_{l'}^{\beta} = 0.$$

Together with eq. (2.10) in the limit, that q goes to zero and the condition for the acoustic out – of – plane branch (eq. (2.17)) we obtain:

$$\frac{\partial^2}{\partial q_\alpha \partial q_\beta} |[D_{zz}(1,1,q) + D_{zz}(1,2,q)]|_{q=0} = 0$$

This means that the right hand side of eq. (2.17) starts with terms of order q^4, so $\omega_{ZA}(q) \propto q^2$ for $q \to 0$. The rotational invariance of a two – dimensional crystal for in – plane rotations implies that the acoustic out – of – plane mode has a quadratic dispersion near the zone center.

ii. Theory of Elasticity for Thin Plates

Another way to calculate the behaviour of the dispersion relation for out – of – plane waves is from the theory of elasticity for thin plates. Landau and Lifshitz [9] explained how the theory of elasticity provides the free energy of a bent plate. This theory is valid for thin plates, where the thickness h is small compared to the dimensions in the other two directions. In a thin plate, bent by external forces, as in figure 2.1, we denote the vertical displacement of a point on the neutral surface (the surface that lies midway through the plate) with ζ. We assume that the deformations are small. In [9] the free energy for a thin plate is calculated as a function of the deformations.

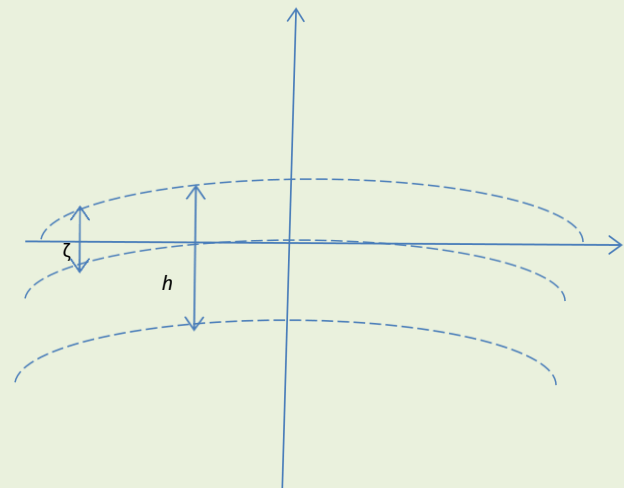

Figure 2.1: A thin plate bent by external forces

It can be derived the equation of equilibrium from the condition for the minimum of the free energy. The equation of equilibrium for a thin plate bent by external forces P

is:

$$\frac{Eh^3}{12(1-\sigma^2)}\Delta^2\zeta - P = 0$$

where E is Young's modulus and Poisson's ratio is σ. The two-dimensional Laplacian is Δ.

If we replace the force by the acceleration $-P \rightarrow \rho h\frac{\partial^2\zeta}{\partial t^2}$, where ρh is the mass per unit area, we find the equation of motion:

$$\rho\frac{\partial^2\zeta}{\partial t^2} + \frac{Eh^2}{12(1-\sigma^2)}\Delta^2\zeta = 0 \qquad (2.18)$$

For waves, we can take the ansatz $\zeta \propto e^{i(q.r-\omega t)}$ and substitute it in the equation of motion eq. (2.18). This implies directly that $\omega^2(q) \propto q^4$ for the bending waves with long wavelengths in the thin plate.

2.2.3. Flexural Phonons in a Strained Sample

Lifshitz [5] showed that in two – dimensional materials, $\omega_{ZA}^2(q)$ is quartic in q near the zonecentre, but gains a quadratic term when there is strain in the sample. The dispersion relation $\omega(q)$ of the acoustical out – of – plane mode with strain written as:

$$\omega_{ZA}^2(q) = \frac{k}{\rho}|q|^4 + u\frac{2(\boldsymbol{\lambda}+\boldsymbol{\mu})}{\rho}|q|^2 \qquad (2.19)$$

where κ is the bending rigidity, ρ is the density; u is the uniform dilatation of the crystal, and λ and μ are the Lamé coefficients. Without strain, the second term would be zero and the mode $(\omega\ (q))$ would be purely quadratic form and takes the following form $\omega(q) = \sqrt{\frac{k}{\rho}}\ |q^2|$. From the dispersion close to $q \rightarrow$ *zero* of the acoustic out – of – plane mode one can calculate the bending rigidity κ.

3 EMPIRICAL POTENTIAL

Calculating the phonon dispersion relation can be done in different ways. There are two starting points for computational methods. The first one is to start from elementary equations like the Schrödinger equation and calculate the quantities needed. Therefore, this method is called *ab initio* or from first principles. The second one uses an empirical potential, which gives the energy of a certain configuration of atoms. This potential is based on a model and on certain parameters. The advantage of using an empirical potential is that it allows one to calculate much larger samples, since it is computationally less time-consuming than *ab initio* calculations.

The empirical potential we use in this paper is a long – range bond order potential, namely LCBOP developed by J.H. Los and A. Fasolino. This chapter introduces this potential.

3.1. (LCBOP)

LCBOP is a bond order potential [10]. This type of potential can describe different-bonding states of the atom. It assumes that the strength of a chemical bond depends on the bonding environment of the atoms. This type of potential is so – called force field that can describe the energy variations only around equilibrium. Bond order potentials allow changes of coordination and bond formation and breaking. LCHBOP describes all phases of carbon and transitions among them with good accuracy [11].

The long – range carbon bond order potential (LCBOP) [1] has a short range and along range part, (a later version includes a medium range term [12]. The long – range part is a Morse like potential. The short – range part contains a number of modifications as compared to the Brenner potential [13]. There are different models for deciding when the long – range part should be switched off. In this potential, the long – range interactions are only excluded for nearest neighbours.

The potential calculates the total binding energy of a configuration of atoms, given by:

$$E_b = \frac{1}{2}\sum_{ij}^{N} V_{ij}^{tot} = \frac{1}{2}\sum_{i,j}^{N} (f_c(r_{ij})V_{ij}^{SR} + S(r_{ij})V_{ij}^{LR}$$

The total pair interaction V_{ij}^{tot} is given as a sum of the short – range interaction V_{ij}^{SR} and the long – range interaction V_{ij}^{LR}, for different distances between the atoms:

The short range part is bond order potentials

$$V_{ij}^{sr} = V_{ij}^{r} + B_{ij}V^{a}$$

this bond order B_{ij} is defined as

$$B_{ij} = \frac{1}{2}\left(b_{ij} + b_{ji}\right) + F_{ij}^{*} + A_{ij} + T_{ij}$$

where b_{ij} is described as the angular dependence of bonds, A_{ij}, is described as the anti bonding states, T_{ij}, describes torsional effect and F_{ij}^{*} describes as the conjugation term which describes the (effective) number of electrons in the bond.

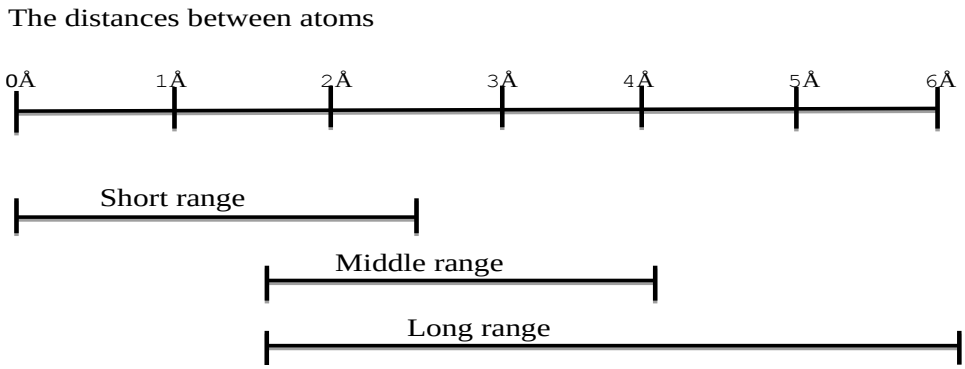

Figure 3.1 the distances between atoms

The short-range interaction describes the covalent bonds. In this term, the bond order character of the potential is included. The long – range interaction accounts for the non – bonded interactions. Later a middle range term is included, which takes into account the rest of the attractive interactions in the middle range regime. These attractive interactions are also environment-dependent. The function $f_c(r_{ij})$ is a smooth cut off function and $S(r_{ij})$ excludes only the nearest neighbors.

3.2. Tight Binding Approximation

The energy band dispersion of graphene can be calculated using a tight-binding model for electrons hopping in the honeycomb lattice. In this approximation we consider only hopping between nearest neighbor atomic sites since the energy contribution from the higher order hopping terms is small [32].

In this section we will present only the essential mathematical steps which lead to the graphene dispersion relation. We will refer the interested reader to [33] and [31] references for more details.

In order to derive the band structure of graphene *(E- k)* relation we solve the Schrödinger equation as follows:

$$\hat{H}\psi = E\psi \tag{3.1}$$

where $\hat{H}$ is the Hamiltonian, ψ is the total wave function, and E is the energy of electrons in the orbital of graphene [33]. As we said graphene lattice has two carbon atoms, A and B, per unit cell [28]. So the total wave function ψ can be written as a linear combination of two Bloch functions u_A and u_B as follows:

$$\psi(\vec{k},\vec{r}) = c_A u_A(\vec{k},\vec{r}) + c_B u_B(\vec{k},\vec{r}) \tag{3.2}$$

by substituting Eq. (3.2) in Eq. (3.1), multiplying by the complex conjugate of u_A^* and u_B^* and integrating over the entire space, we can write the Schrödinger equation in (3.1) in matrix form as follows:

$$\begin{pmatrix} H_{AA} & H_{AB} \\ H_{BA} & H_{BB} \end{pmatrix} \begin{pmatrix} c_A \\ c_B \end{pmatrix} = E \begin{pmatrix} S_{AA} & S_{AB} \\ S_{BA} & S_{BB} \end{pmatrix} \begin{pmatrix} c_A \\ c_B \end{pmatrix} \tag{3.3}$$

where the matrix elements are defined as follows.

$$H_{ij} = \int_\Omega u_i^* \hat{H} u_j dr,\ S_{ij} = \int_\Omega u_i^* u_j dr$$

H_{ij} , is the matrix elements of the Hamiltonian or transfer integral, S_{ij} the overlap matrix elements between Bloch functions.

Since the atoms A and B in the unit cell of the graphene are identical the matrix elements are taken to be equals such that $H_{AA} = H_{BB}, S_{AA} = S_{BB}$ [31], and the overlapping between wave functions of different atoms is neglected. i.e. $S_{BA} = S_{AB} = 0$, while $S_{AA} = S_{BB} = 1$ [33].

To get a non-trivial solution for Eq. (3.3), the determinant of this matrix must vanish, namely:

$$\begin{vmatrix} H_{AA} - E & H_{AB} \\ H_{BA} & H_{BB} - E \end{vmatrix} = 0 \tag{3.4}$$

the solution of this determinant gives us the Eigen energies in terms of the matrix elements:

$$E = H_{AA} \pm |H_{AB}| \tag{3.5}$$

to evaluate the matrix elements which are given in Eq. (3.5) the wave functions u_A and u_B are taken as a linear combination of wave functions localized at each atom site:

$$u_{A(B)}(\vec{k}, \vec{r}) = \frac{1}{\sqrt{N}} \sum_{A(B)}^{N} e^{i\vec{k}\cdot\vec{r}_{A(B)}} X\left(\vec{r} - \vec{r}_{A(B)}\right) \tag{3.6}$$

where $X(\vec{r})$ is the orbital $2P_z$ wave function for an isolated carbon atom, N is the number of the unit cells [33].

We can calculate the diagonal matrix elements ($H_{AA} = H_{BB}$) as follows:

$$H_{AA} = \frac{1}{N} \sum_{A} \sum_{A^*} e^{i\vec{k}\cdot(\vec{r}_A - \vec{r}_A^*)} \int X^*(\vec{r} - \vec{r}_A)\, HX(\vec{r} - \vec{r}_A^*)\, d\tau \tag{3.7}$$

for calculating the matrix elements given by Eq. (3.7) we consider the effect of the three nearest neighbors for each atom A (B):

$$H_{AA} = \int X^*(\vec{r} - \vec{r}_A) HX(\vec{r} - \vec{r}_A^*) d\tau = E_0 = H_{BB} \tag{3.8}$$

$$H_{AB} = \frac{1}{N} \sum_{A} \sum_{B^*} e^{-i\vec{k}\cdot(\vec{r}_A - \vec{r}_B)} \int X^*(\vec{r} - \vec{r}_A)\, HX(\vec{r} - \vec{r}_B)\, d\tau \tag{3.9}$$

$$H_{AB} = \frac{1}{N} \sum_i e^{-i\vec{k}\cdot\vec{R}_l} \int X^*(\vec{r})\, HX(\vec{r} - \vec{R}_l)\, d\tau \tag{3.10}$$

where $\vec{R}_l$ is a vector connecting atom A to its three nearest neighbor B atoms as shown early in chapter one section 1.1 and 1.2.

Eq. (3.10) becomes:

$$H_{AB} = (e^{-i\vec{k}\cdot\vec{R}_1} + e^{-i\vec{k}\cdot\vec{R}_2} + e^{-i\vec{k}\cdot\vec{R}_3}) \int X^*(\vec{r})\, HX(\vec{r} - \vec{R}_l) d\tau \tag{3.11}$$

where $\int X^*(\vec{r})\, HX\left(\vec{r}-\vec{R}_l\right)d\tau = \gamma_0$ is the transfer integral or the nearest neighbor interaction.

Eq. (3.11) becomes:

$$H_{AB} = (e^{-i\vec{k}\cdot\vec{R}_1} + e^{-i\vec{k}\cdot\vec{R}_2} + e^{-i\vec{k}\cdot\vec{R}_3})\gamma_0 \qquad (3.12)$$

The matrix element H_{AB} can be calculating directly by substituting the values of the coordinates of the nearest neighbor vectors $\vec{R}_l$ $(i = 1, 2, 3)$ in Eq. (3.12).

$$E = E_0 \pm |H_{AB}| = E_0 \pm \sqrt{H_{AB}H_{AB}^*}$$

$$= E_0 \pm \gamma_0 \left[1 + 4\cos\left(\frac{\sqrt{3}}{2}k_x a\right)\cos\left(\frac{k_y a}{2}\right) + 4\cos^2\left(\frac{k_y a}{2}\right)\right]^{\frac{1}{2}}, \qquad (3.13)$$

where $a = \sqrt{3}a_{cc} = \sqrt{3}a_0$.

For the sake of simplicity, we rewrite the dispersion relation in terms of the new parameters $a = \left(\frac{3a}{2}\right)$, and $b = \left(\sqrt{3}\frac{a_0}{2}\right)$ as follows:

$$E = E_0 \pm \gamma_0 \left(1 + 4\cos(k_x a)\cos\left(k_y b\right) + 4\cos^2\left(k_y b\right)\right)^{\frac{1}{2}} \qquad (3.14)$$

The negative and positive signs in Eq. (3.14) refer to the valance and conduction bands respectively [36].

The main feature of the energy dispersion of graphene as we will see in the next chapter is the six points at the corners of the Brillouin zone, where the conduction and valance bands meet so that, the band gap is zero only at these points [33].

The six points are also the points at which the Fermi energy cuts two bands and so the solid has six Fermi points [30]. Even more interesting is the form of the valance and conduction bands close to Dirac points, they show a conical shape, with negative (valance) and positive (conduction) energy values [29] as we are going to show in the coming sections.

If we return to the high symmetry points like $\boldsymbol{\Gamma}$, $\boldsymbol{M}$ and $\boldsymbol{K}$ and substitute their coordinates in Eq. (3.13) we can see that at $\boldsymbol{\Gamma}$- points, such as $\vec{k} = \frac{2\pi}{\sqrt{3}}\hat{k}_x$, the bands are separated by $2\gamma_0$. The vector $\vec{k}$ of one of $\boldsymbol{K}$- points is $\overrightarrow{\Gamma k} = \frac{1}{3}\left(2\vec{b}_1 + \vec{b}_2\right) = \frac{2\pi}{\sqrt{3}}\hat{k}_x + \frac{2\pi}{3a}\hat{k}_y$ gives $E_g = 0$. So, at the k and, k'ponts, the two bands touch and they

called Dirac points [35].

In order to find the Dirac points coordinate we make the determinant of the transfer integral vanishes such that $|H_{AB}| = 0$ in Eq. (3.14) where the eigenvalue $E = \pm|H_{AB}|$ [34]. Taking $E_0 = 0$, and let $H_{AB} = h'(\vec{k})$ for simplicity, this lead to the following root equation:

$$\left|h'(\vec{k})\right| = \gamma_0 \left(1 + 4\cos(k_x a)\cos(k_y b) + 4\cos^2(k_y b)\right)^{\frac{1}{2}} = 0$$

for $k_x a = 0$ we have:

$$\left|h'(\vec{k})\right| = \gamma_0 (1 + 2\cos(k_y b)) = 0 \text{ and } k_y b = \pm\frac{2\pi}{3}.$$

these six points are special as they provide the states right around the Fermi energy and thus determine the electronic properties. They can be put into two groups; each group has three points as follows:

$$(k_x a, k_y b) = \left(0, \frac{2\pi}{3}\right), \left(-\pi, -\frac{\pi}{3}\right), (\pi, -\frac{\pi}{3})$$

$$(k_x a, k_y b) = \left(0, -\frac{2\pi}{3}\right), \left(-\pi, \frac{\pi}{3}\right), (\pi, \frac{\pi}{3})$$

All three within group are equivalent point since they differ by a reciprocal lattice vector as shown in Fig. 3.2. Each group gives $(k_x a, k_y b) = \left(0, \pm\frac{2\pi}{3}\right)$.

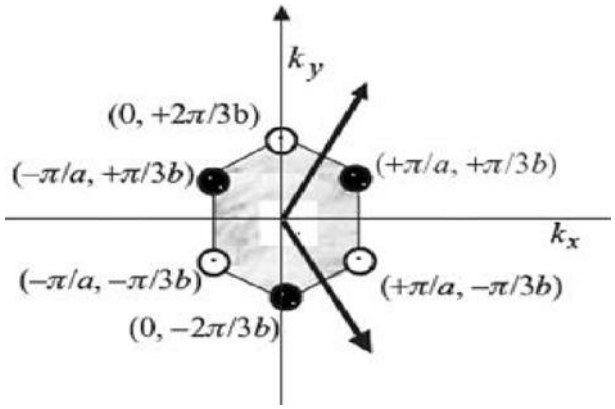

Fig. 3.1: The special points of graphene first Brillouin zone [34].

3.3. The Energy Dispersion Relation of Graphene

3.3.1. The Dispersion Relation as Function of k_x and k_y

The numerical values of the energy of the graphene in the dispersion relation given by Eq. (3.13) had been calculated and displayed numerically in Fig. 3.3 with $E_0 = 0$. Our results obtained in Fig. 3.3 are in agreement with the standard results reported by [31].

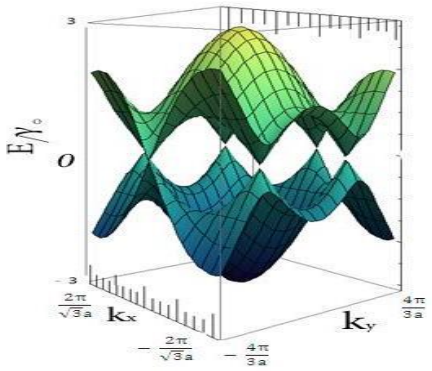

Fig. 3.3: The scaled energy as function of k_x and k_y of graphene reproduced fro ref. [31].

3.3.2. The Dispersion Relation as Function of k_y

To show the behavior of the graphene near the Dirac point, we have used both the exact dispersion relation, Eq. (3.13), and the approximate results, to obtain the numerical results of the energy against the wave vector as shown in Fig. 3.3. The Figure clearly shows the linear behavior of the dispersion relation close to the Dirac points and displays our calculated results against the standard results reported in [34].

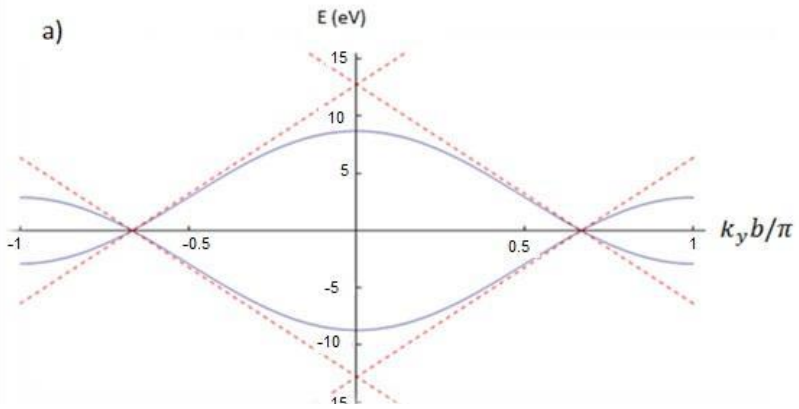

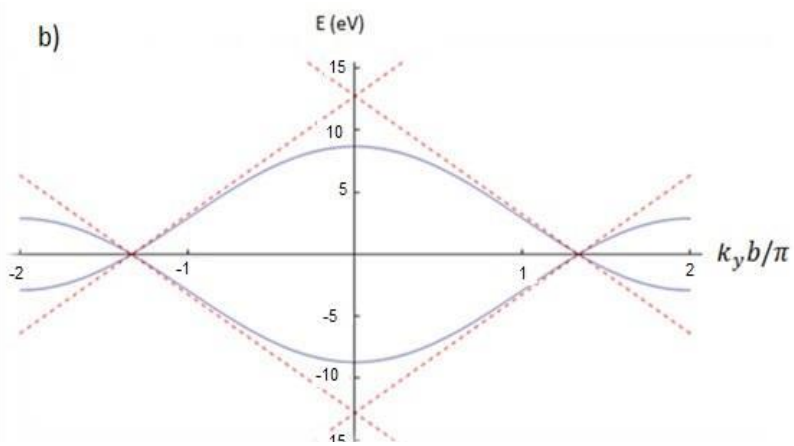

Fig. 3.4: The energy (in eV) of the graphene for arbitrary k_y values and particular restricted k_x values ($k_x a = 0$). The dashed curve represents the behavior of the dispersion relation near the Dirac points, while the solid line represents the behavior of the exact dispersion relation Eq. (3.1 3). a) Our results compared against the standard ones [34]. b) Our results calculated for extended $k_y b$ range.

4 HARMONIC APPROXIMATION

In this chapter I reviewed briefly the methods used by Karssemeijer and Fasolino [4] for calculating the phonon dispersion relation in graphene. They used the theory of lattice dynamics as explained in section 2.1. This is a purely harmonic theory. For their calculation, they used the empirical potential LCBOP, described in section 3.1.

Therefore, this mode could be strongly temperature dependent and we have to include anharmonic effects. Then, we will look what the effect of strain is on the ZA-branch in the harmonic approximation.

4.1. Flexural Phonon Mode under Strain

In this section, we will look how the phonon dispersion relation of the ZA – mode behaves under strain. All calculations are done in the harmonic approximation. In section 2.3.2 the relation between the acoustic out of plane mode and the bending rigidity was explained. In this section, we will look in more detail at what this implies.

We calculated the phonon dispersion relation for different lattice parameters or, in other words, under different strains. For easy reading, we repeat the equation for the acoustic out of plane mode that was explained in section 2.3.2:

$$\omega^2(q) = \frac{k}{\rho}|q|^4 + u\frac{2(\lambda+\mu)}{\rho}|q|^2 \qquad (4.1)$$

In figure 4.1 we show the acoustic out of plane mode for graphene with a lattice parameter a = 1.4195 Å. This is slightly smaller than the equilibrium lattice parameter at T = 0K: $a_{(T=0K)} = 1.4198\text{Å}$. We see that this gives some imaginary frequencies, since the second term in equation (4.1) is negative and dominant over the first term for small q. In order to fit the phonon dispersion relation with equation (4.1), in figure 4.2, we show the behaviour of the fitting parameters. With increasing lattice parameter, the bending rigidity decreases and seems to scale linearly with the lattice parameter. The quadratic term (due to strain) increases with increasing lattice parameter and is zero for the equilibrium lattice parameter. From that we see that at equilibrium lattice parameter and for T = 0K, the bending rigidity is κ = 0.66eV.

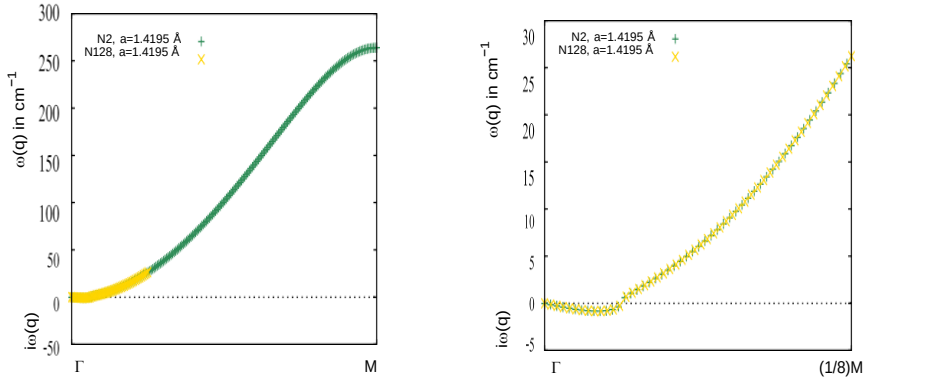

(a) Dispersion relation $\omega_{ZA}(q)$ from Γ to M (b)Detail: dispersion relation $\omega_{ZA}(q)$ from Γ to $\frac{1}{4}M$

Figure 4.1: in 4.1 (a) and (b), the dispersion relation is plotted from Γ to M in the Brillouin zone of the unit cell with two atoms. For our super cell with 128 atoms, the Brillouin zone folds in eight parts in this direction. From now on we will look at the path from Γ to $\frac{1}{8}M$ showed by the yellow (light grey) points in the left graph and explicitly given in the right graph.

4.2. Quasiharmonic Approximation

In the theory of lattice dynamics that we derived in section 2.1, we used the harmonic approximation. In the harmonic approximation, the vibrations in the crystal are independent of the inter-atomic distance. This directly implies that the vibrational energy does not depend on volume and so the equilibrium lattice parameter does not depend on temperature. Actually, nothing depends on temperature, since temperature is not at all included in the harmonic approximation. A proper way to consider the anharmonic effects is to calculate all anharmonic terms, but this is not a reasonable task. A simple way to consider some anharmonic effects for calculations of the free energy is the quasi – harmonic Approximation (QHA). This chapter will introduce the theory of the quasi-harmonic approximation. It provides two ways to calculate the thermal expansion coefficient. With these two ways, the thermal expansion coefficient for graphene will be calculated and compared to the DFT calculations of Mounet and Marzari [19].

4.2.1. Theory: Quasi-Harmonic Approximation

In the quasiharmonic approximation, we use the harmonic partition function but we assume that the frequencies depend on the volume (global constraints(X)).

The free energy can be calculated from the partition function. The partition function

consists of a part due to the static lattice energy and a part due to the vibrations, which are in the harmonic approximation 3N independent oscillators. The (harmonic) partition function Z due to the vibration contribution is given by:

$$Z = \prod_{qj} Z_{qj} = \prod_{qj} \left[\sum_{n=0}^{\infty} e^{-\frac{\hbar\omega_{qj}}{k_B T}\left(n+\frac{1}{2}\right)} \right]$$

$$= \prod_{qj} \left[e^{-\frac{\hbar\omega_{qj}}{k_B T}} \left(1 - e^{-\frac{\hbar\omega_{qj}}{2k_B T}} \right)^{-1} \right] \qquad (4.2)$$

For the free energy in the quasiharmonic approximation, one assumes that the frequencies are dependent on the global constraint *X*, so $\omega_{qj} \rightarrow \omega_{qj}(X)$. Furthermore, one has to include the zero temperature energy of the crystal $U_0(X)$ since it is volume dependent.

The free energy is then obtained by substitution of the partition function expression in the well-known formula:

$$F = -k_B T ln(Z)$$

Giving as a final expression: the free energy in the quasiharmonic approximation become

$$F(X,T) = U_0(X) + \frac{1}{2}\sum_{qj} \hbar\omega_{qj}(X) + k_B T \sum_{qj} \ln\left(1 - e^{-\frac{\hbar\omega_{qj}(X)}{k_B T}} \right) \qquad (4.3)$$

where q, j sums over all wave vectors q and their branches j in the Brillouin zone. Note that *X* is usually the volume, but it can also contain anisotropic components of the strain tensor, some external applied fields, or distortions of the crystal lattice. When we take for *X* the volume we can calculate many thermodynamic quantities like the Grüneisen parameters. Where the first term is internal contribution, the secondly term and third term is the zero point and vibration contribution respectively. The phonon frequency is only determined by volume and independent of the temperature in quasiharmonic approximation.

Whether the quasiharmonic approximation is enough to describe the system depends on the system and can only checked by calculations.

The quasiharmonic approximation can be useful to calculate the temperature

dependence of thermodynamic quantities like the thermal expansion coefficient, the Grüneisen parameters, and the heat capacity. In this reviewed papers we will look especially at the thermal expansion coefficient since the thermal expansion coefficient of graphene is strongly temperature Dependent [19], [20]. Moreover the thermal expansion coefficient of graphene is, unlike for most materials, negative at temperatures below about 800K. This is a feature of membranes or layered materials (like graphite). One can intuitively understand the negative thermal expansion coefficient in the following way: for finite temperatures, membranes start to ripple. The deformations in the *z* – direction cause in – plane strain, which causes the area to decrease. It proposed [20] that the lattice parameter of graphene first decreases and then above ~ 1000K increases. This illustrates why the thermal expansion coefficient of graphene is very unusual.

4.2.2. Thermal Expansion Coefficient

The thermal expansion coefficient can be calculated in two ways within the quasiharmonic approximation [19]. The first one is to minimize the quasiharmonic free energy (eq. (4.3)) for each temperature in the lattice parameter. This gives for each temperature a lattice parameter *a* (T) where the free energy has a minimum.

Once we have calculated the lattice constant, we will go one-step further and work out the thermal expansion coefficient $\alpha(T)$. This is given by the linear thermal expansion coefficient α can be calculated by:

$$\alpha(T) = \frac{1}{a(T)}\frac{da(T)}{dT}$$

For graphene we have of course only two dimensions and moreover, the lattice parameter depends only on one lattice parameter a. For a structure with only one lattice parameter the condition $(\frac{\partial F}{\partial a})_T = 0$ leads to (as explained for example in [23])

$$\alpha = \frac{1}{{a_0}^2 \frac{\partial^2 U_0}{\partial a^2}\Big|_0} \sum_{qj} C_v(qj) \frac{-a_0}{\omega_0(qj)(X)} \frac{\partial \omega_{qj}(X)}{\partial a}\Big|_0 \qquad (4.5)$$

where U denotes the potential energy and the subscript 0 indicates that the quantity is taken at the equilibrium lattice parameter. The quantity $C_v\ (qj)$ is the contribution to the specific heat from mode (q, j). The total heat capacity per unit cell at constant volume can be calculated as:

$$C_v = -T\left(\frac{\partial^2 F_{vib}}{\partial T^2}\right)_v$$

Where F_{vib} is the vibration part of the free energy and is given by the last term of equation (4.3). By taking the second derivative with respect to temperature, we obtain:

$$C_v = -\sum_{q,j}\left(\frac{\hbar\omega_{qj}(X)}{2k_BT}\right)^2 \frac{1}{\sin h^2\left(\frac{\hbar\omega_{qj}(X)}{2k_BT}\right)}$$

$$C_v = k_B\left(\frac{\hbar\omega_{qj}(X)}{2k_BT}\right)^2 \left[\sin h^2\left(\frac{\hbar\omega_{qj}(X)}{2k_BT}\right)\right]^{-1}$$

In this section we will calculate the thermal expansion coefficient in the two ways described in section 4.2.2 and compare our results with similar calculations from Mounet and Marzari [19].

4.2.2.1. Direct Minimisation of the Free Energy

In this subsection, we calculate the thermal expansion coefficient by minimising the free energy for every temperature with respect to the lattice parameter. We do this in the following way: for each temperature, we calculate the quasiharmonic free energy for several lattice parameters, as is shown for T = 20K in figure 4.3. We performed the calculations for 67 temperatures from 5K in steps of 5K and for 50 different lattice parameters between 1.4198 Å and 1.4298 Å in equal steps.

In order to find the minimum of the free energy for a given temperature with respect to the lattice parameter, we fitted a polynomial to the free energy and calculated the minimum of the polynomial. The order of the polynomial and the fitting range influence the behaviour of the lattice parameter as shown in graph 4.4 (a). The thermal expansion coefficient was calculated by fitting a polynomial (up to 5th order) to the data for $a_{cc}(T)$. From this fit we calculated by $\alpha(T) = \frac{1}{a(T)}\frac{da(T)}{dT}$.

For low temperatures, there is a good agreement between the different fitting methods for the nearest neighbour distance. For higher temperatures the different fitting methods give different results and we cannot say anything about the shape of the thermal expansion coefficient α.

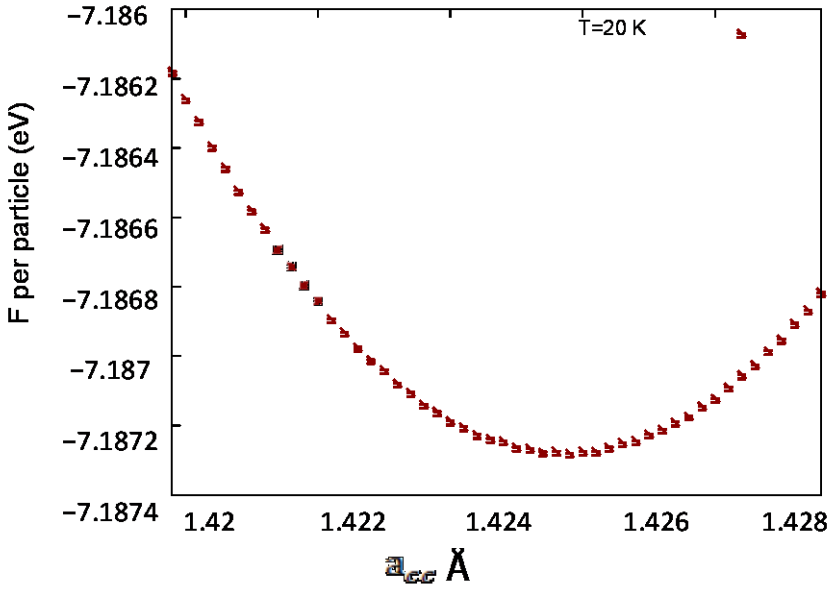

Figure 4.2: Quasiharmonic free energy for graphene at T = 20K as a function of the lattice parameter [26].

4.2.2.2. Grüneisen Formalism

In this subsection we calculated the thermal expansion coefficient with the grüneisen formalism as explained in section 4.2.2. The calculation of the phonon dispersion relation, its derivatives with respect to the lattice parameter and the second derivative of the static lattice energy with respect to the lattice parameter are calculated with LCBOP, via the method explained in section 2.1.

There are two possibilities for the equilibrium lattice parameter that only differ by the zero point motion: the lattice parameter that minimises the energy or the one that minimises the free energy at T = 0K, namely including zero point motion [26]. The lattice parameter that minimizes the energy is $a_{cc}^{U_{min}}$ = 1.4198 ˚A and the lattice parameter that minimizes the free energy is $a_{cc}^{F_{min}} = 1.4257$ Å.

We cannot perform the calculations at exactly $a_{cc}^{U_{min}}$, since for the derivatives we need to calculate the dispersion relation in $a_{cc} = a_{cc}^{U_{min}} - \epsilon$. For lattice parameters smaller than $a_{cc}^{U_{min}}$ the dispersion relation has imaginary frequencies, which is unphysical. Therefore we calculated the thermal expansion coefficient with the Gru¨neisen formalism for an equilibrium lattice parameter of $a_{cc}^{U_{min}}$ = 1.4198 + 0.0002 = 1.4200 ˚A. This is nearly the lattice parameter that minimizes the energy. Moreover we calculate the thermal expansion coefficient for a lattice parameter that

minimizes the free energy $a_{cc}^{F_{min}} = 1.4257$ ˚A.

When the thermal expansion coefficient calculated with equation eq. (4.8) and one knows the initial lattice parameter one can obtain the lattice parameter depending on the temperature $(a_{cc}(T))$ by integrating eq. (4.7). The thermal expansion coefficient and the lattice parameter are plotted in figure 4.5.

4.3. Comparing Different Methods

In this subsection we compare our methods with each other and with calculations done by Mounet and Marzari [19]. Remarkably there are considerable differences among the methods.

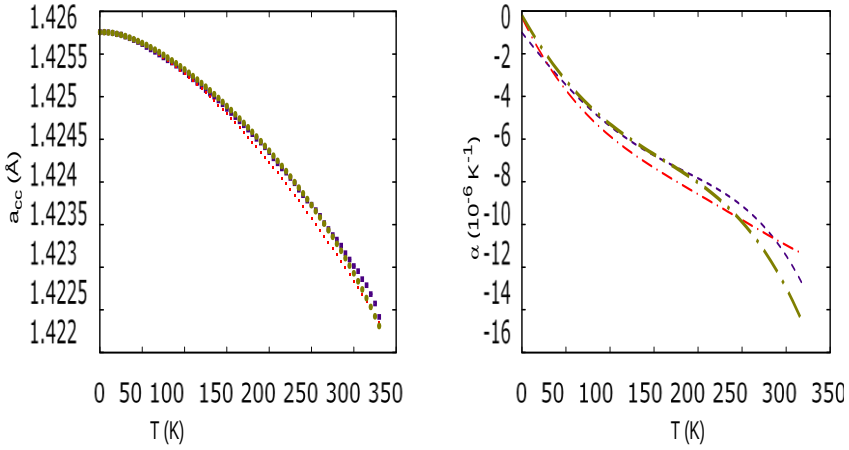

(a)Nearest neighbour distance [26] (b) Thermal expansion coefficient [26]

Figure 4.3: The minimum of the free energy is found by fitting a polynomial to the free energy and calculated. For the red crosses (dot-dashed line), a quadratic polynomial was used and the fit was performed over the whole range. For the green dots (line with squares and stripes) a cubic polynomial was used and the fit was again performed over the whole range. For the purple squares (fine dotted line) a quadratic polynomial was used and the fit was first performed over the whole range which gave an initial minimum, but secondly the fit was redone over a range of 0.002Å around the initial minimum. We see that up to around 100K the three methods agree reasonable for the nearest neighbour distance. Above 100K, the different fitting methods give different results and we cannot say anything about the shape of α [26].

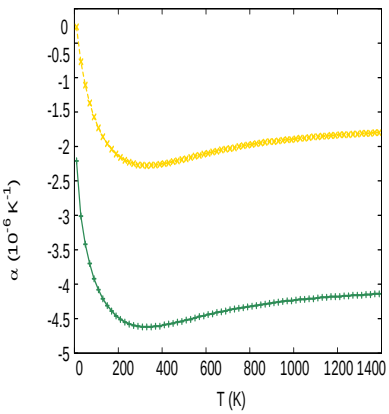

(a) Thermal expansion coefficient [26]

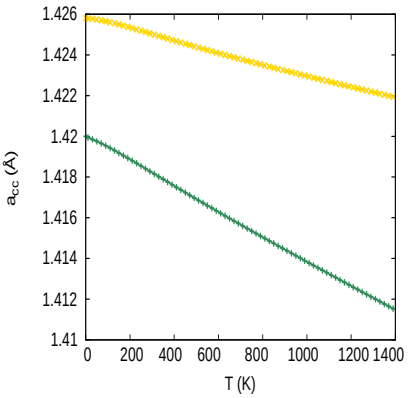

(b) Nearest neighbour distance Å [26]

Figure 4.4: The yellow (light grey) lines represent the calculation for $a_{cc}^{F_{min}}$ = 1.4257Å. The green (dark grey) lines the calculations for $a_{cc}^{U_{min}}$ = 1.4198 + 0.0002Å = 1.4200Å. This figure is reproduced from ref. [26]

In all cases, the lattice parameter decreases with increasing temperature. The curve for the thermal expansion coefficient that Mounet and Marzari obtained via direct minimization of the free energy mostly resembles our calculations via the Gru¨neisen formalism. We find a quite large and negative thermal expansion coefficient in our calculations via direct minimization of the free energy.

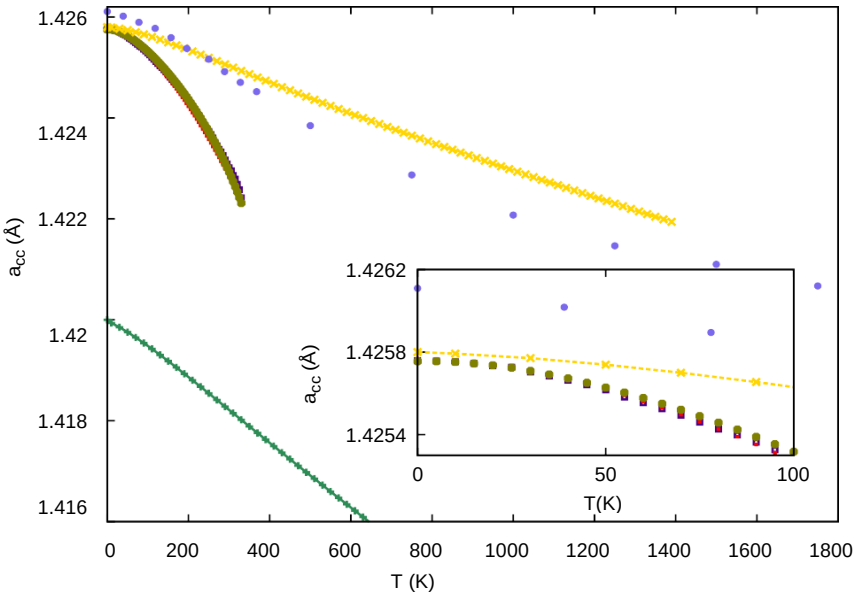

(a) Nearest neighbour distance (26)

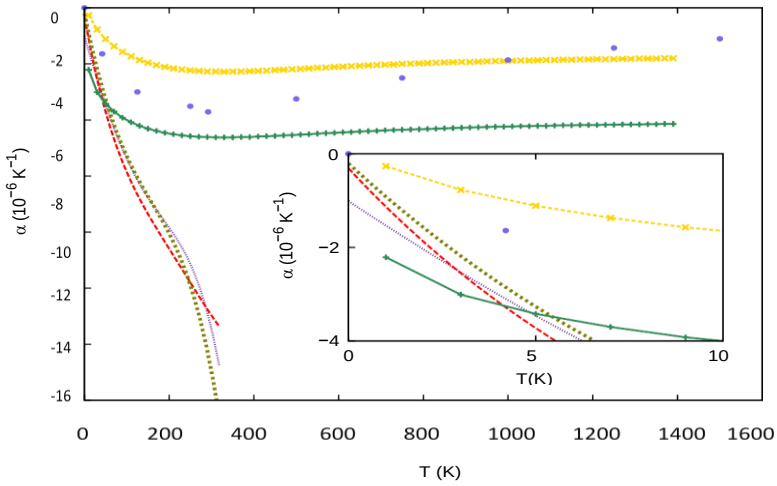

(b)Thermal expansion coefficient (26)

Figure 4.5: The color scheme of these diagrams are the same as for the previous figures in this section: nearest neighbor distance calculated by minimizing the free energy: red crosses/dot-dashed line (fitted with quadratic polynomial over the whole range), olive green dots/line with squares and stripes (fitted with cubic polynomial over the whole range), purple squares/fine dotted line (fitted with quadratic polynomial around the minimum). Thermal expansion coefficient calculated via the Grüneisen formalism: yellow crosses/dashed line ($a_{cc}^{F_{min}}$), dark – green pluses/solid line ($a_{cc}^{U_{min}}$) [26]. The additional light-purple round dots approximate the computational data from Mounet and Marzari [19]. They used the minimization of the free energy for their calculations of the nearest neighbor. They calculated the thermal expansion coefficient by differentiation.

4.4. Comparing the different Temperatures

In our study, we are interested in the temperature dependence, for a reason we evaluate in this section if there are any differences between the calculated phonon dispersions for the different temperatures. We begin with a general discussion and then derive the temperature dependence of the bending rigidity (k) and then calculated phonon dispersions of graphene.

It is difficult to compare the phonon dispersions at different temperatures directly from different figures (4.6, 4.7, and 4.8); therefore, we made one combined graph of all the dispersion results for all the different temperatures as shown in figure 4.9. Now we are able to see some differences for the optical modes. It is clearly visible that the optical modes for the different temperatures deviate more from each other than the acoustic modes. For example the TO shifts by about $\Delta\omega \approx 100\text{cm}^{-1}$, which is an enormous difference. This can also be seen in the below figures, especially the phonon frequency at $\omega\,(\text{cm}^{-1})$, which is the phonon frequency for the double

degenerate TO and LO mode at Γ, is in our interest.

We can compare these data namely to the study of E.N. Koukeraset Al. [25] which more focused on the behaviour of these optical modes. The only difference is that the behaviour of $\omega\,(\mathrm{cm}^{-1})$, which we found, softens a bit harder for temperatures higher than T = 900K. However, this last fact can be explained by the fact that we used another potential and because we only compared 4 different temperatures whereas [25] evaluated 7 different temperatures. These results predict that the optical phonons of graphene are temperature dependent.

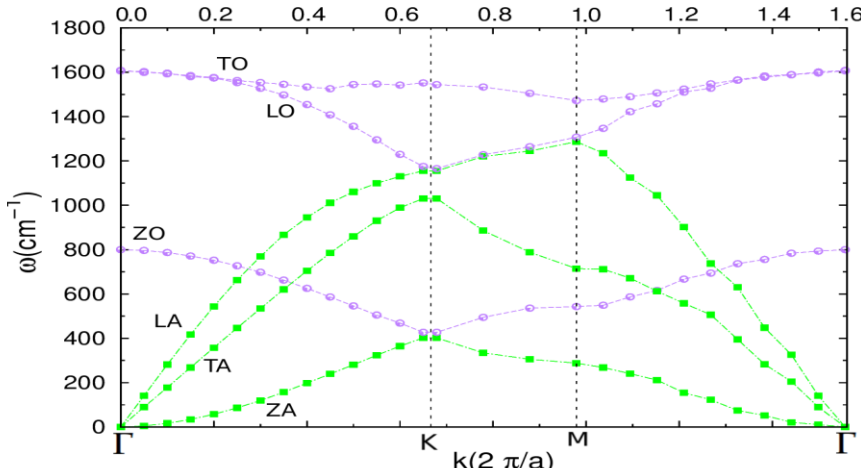

Figure 4.6: Phonons of our 800 – atom graphene sheet for all branches at T = 100K. Based on MD simulations with time step $\Delta t = 0.05 fs$ [27].

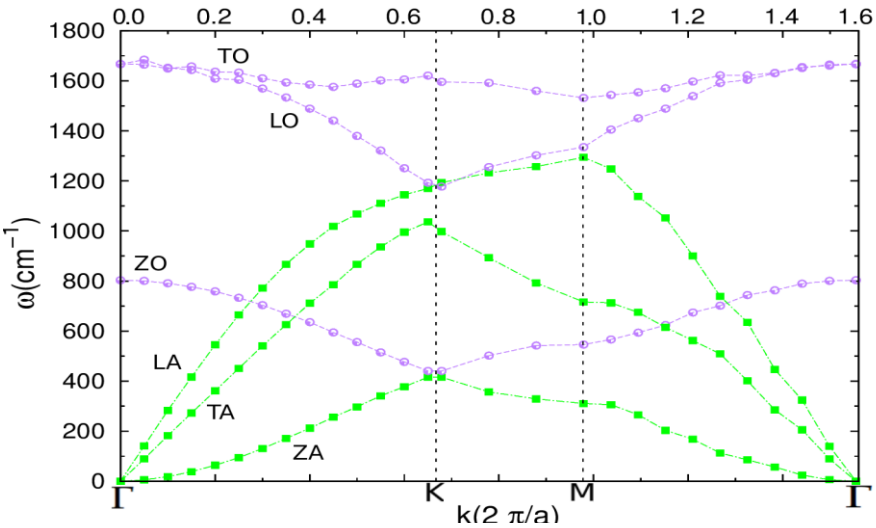

Figure 4.7: Phonons of our 800 – atom graphene sheet for all branches at T = 300K. Based on MD simulations with time step $\Delta t = 0.05 fs$ [27].

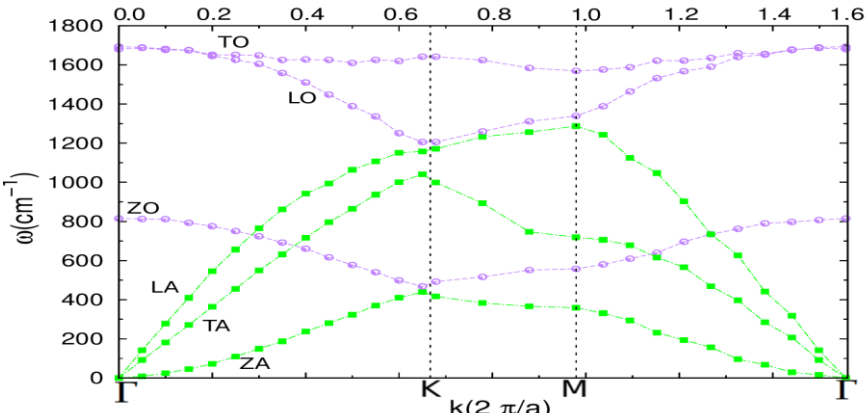

Figure 4.8: Phonons of our 800 – atom graphene sheet for all branches at T = 1000K. Based on MD simulations with time step $\Delta t = 0.05 fs$ [27]

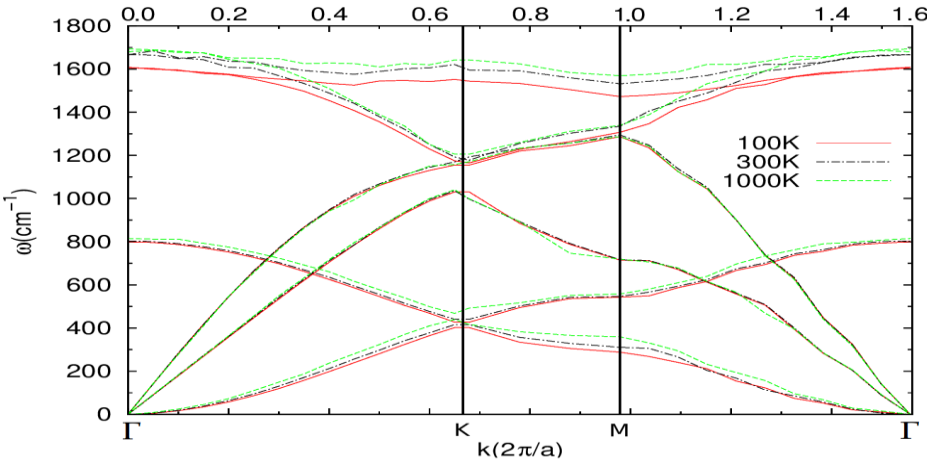

Figure 4.9: Combined graph of figures 4.6, 4.7 and 4.8 which shows the differences between the phonons of graphene at T = 100 K, T = 300 K and T = 1000 K.

4.4.1. Temperature Dependence of the Bending Rigidity

As said and showed in figure 4.10, the in-plane acoustic modes, TA and LA, seem to be independent of temperature. Finally, we determine the bending rigidity (k) by fitting a parabola to our dispersion graphs for graphene as discussed in the above section. as one can see, the bending rigidity (k) clearly increases for higher temperatures. Then finally, we have determined the behaviour of this bending rigidity for different temperatures and to easily compare them to other studies. This behaviour looks a bit like a square root.

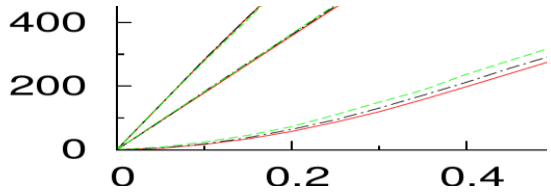

Figure 4.10: Zoom of the temperature difference graph shown in figure 4.10 for the lowest acoustic modes at the lowest k – vectors.

5 CONCLUSIONS

We have studied the temperature dependence of the phonon dispersion relation in graphene with an empirical potential LCBOP that describes the interactions between carbon atoms, also far away from equilibrium structures. These thermal displacements change the frequencies and induce new thermal displacements in the next iteration. Calculating the displacements can be done in various ways.

The strong divergence of the out – of – plane fluctuations in the long wavelength limit for two-dimensional materials has been explained in the harmonic approximation. We neglect the long wavelengths in our calculations of the displacements.

The ZA – mode is characterized by a peculiar quadratic dispersion, which is determined by the bending rigidity κ. From the ZA modes we wanted to compute the temperature dependence of the bending rigidity κ, a coefficient that measure the energy needed to bend the graphene layer. According to the theory of membrane, near the Γ – point, the ZA modes are quadratic in the k – vector, and the coefficient is related to κ, $\omega_{ZA}(k) = \sqrt{\frac{\kappa}{\rho}}\,|k|^2$ we needed to modify the theory to include more effects. For example, we included some strain and modified the relation as follow:

$$\omega_{ZA}(q) = \sqrt{\frac{k}{\rho}|q|^4 + u\frac{2(\lambda+\mu)}{\rho}|q|^2}$$

where $b = 2u(\lambda + \mu)$, with u is the stretching and $\lambda + \mu$ are the Lamé constants. This Equation tells us that we could try to get the bending rigidity using the following fitting function: $\rho\omega^2 = kt^2 + bt$ where $t = q^2$.

The bending rigidity has been found in MC-simulations to depend on the temperature which takes into accounts only coupling between the in – plane and out – of – plane acoustic modes. The fact that the dispersion relation of the za – mode changes with temperature and with iterations, clearly shows that the bending rigidity becomes temperature dependent due to interactions with the whole phonon spectrum. This it is an important conclusion. The determination of the dependence of κ on the temperature, however, has not yet been calculated, because the method is not directly applicable to two – dimensional crystals. Moreover, the lattice parameter of graphene is strongly temperature dependent. Whether graphene is dynamically stable (has only

real frequencies in the harmonic approximation) depends on the lattice parameter. The unknown lattice parameter when we include temperature, and the induced strain due to displacing the atoms out – of – plane, may be a problem. One could think of a method to deal with strain and temperature at the same time.

Graphene is a single layer of carbon atoms densely packed in a honeycomb lattice. The energy structure of crystals depends on the interactions between orbitals in the lattice.

Graphene is a mono atomic layer of graphite with carbon atoms arranged in a two dimensional honeycomb lattice configuration.

Graphene can be used in electronics, transparent displays, power storage, medicine, and so on.

Looking at our results, we found that the optical phonon modes of graphene are strongly temperature dependent by factors of about $\Delta\omega = 100\, cm^{-1}$ when shifting the temperature from T =100K to T = 1000K. We focused on the acoustic phonon branch and we found that the traversal acoustic and the longitudinal acoustic phonon modes are as expected not temperature dependent. These modes turned out to be linear for small wave vectors, as expected according to the theory. What was more interesting is that we found that the out – of – plane ZA mode clearly depends on temperature for small wave – vectors. For small wave vectors the curvature of this mode more than doubled for higher temperatures which is in fact a quite astonishing result.

The most appealing result we got is that the bending rigidity (k), derived from this ZA phonon, increases for higher temperatures.

Finally we want to end this project with an outlook for future research and an explanation of the importance of our findings for the bending rigidity. As said, we still need to improve our results a little, but we have strong indications that the bending rigidity is temperature dependent.

The consequences of this temperature dependent bending rigidity are important when considering elastic response of the materials.

Bibliography

[1] Inka L.M. Locht, "The effect of temperature on the phonon dispersion relation in graphene", *Master thesis,* **2015**.

[2] J. H. Los and A. Fasolino, "Intrinsic long-range bond-order potential for carbon: Performance in montecalrlo simulations of graphitization", Phys. Rev. B, vol. 68, no. 024107, 2003.

[3] P. Souvatzis, O. Eriksson, S. P. Rudin and M. I. Katsnelson, "The self-consistent *ab Initio* lattice dynamical method". Comp. Mat. Sc., vol. 44, pp. 888–894, 2009.

[4] K. S. Novoselov, A. K. Geim, S. V. Morozov, D. Jiang, Y. Zhang, S. V. Dubonos, I. V. Grigorieva, and A. A. Firsov, "Electric field effect in atomically thin carbon films," Science, vol.306, no. 5696, pp. 666–669, 2004.

[5] L. J. Karssemeijer, "Thermal expansion of carbon structures," Master Thesis, http://www.ru.nl/tcm/education_0/bachelor-master/, 2010.

[6] I. M. Lifshitz, Zh. Eksp. Teor.Fiz, vol. 22, p. 475, 1952.

[7] P. Souvatzis, O. Eriksson, S. P. Rudin, and M. I. Katsnelson, "Entropy driven Stabilization of energetically unstable crystal structures explained from first principles theory," Phys. Rev. Lett., vol. 100, no. 095901, 2008.

[8] P. Souvatzis, D. Legut, O. Eriksson, and M. I. Katsnelson, "Ab initio study of lattice Vibrations and stabilization of the _ phase in ni-ti shape-memory alloy," Phys. Rev. B, vol. 81, p. 092201, 2010.

[9] M. Katsnelson, Graphene, Carbon in two dimensions. Cambridge university press, 2012.

[10] L. Landau and E. Lifshitz, Theory of elasticity. Pergamon Press, 1970.

[11] J. Tersoff, "Empirical interatomic potential for carbon, with applications to amorphous carbon". Phys. Rev. Lett., vol. 61, pp. 2879–2882, 1988.

[12] L. M. Ghiringhelli, J. H. Los, E. J. Meijer, A. Fasolino, and D. Frenkel, "Modeling the phase diagram of carbon," Phys. Rev. Lett., vol. 94, p. 145701, 2005.

[13] J. H. Los, L. M. Ghiringhelli, E. J. Meijer, and A. Fasolino, "Improved long-range reactive bond-order potential for carbon. i. construction," Phys. Rev. B, vol. 72, p. 214102, 2005.

[14] D. W. Brenner, “Empirical potential for hydrocarbons for use in simulating the chemical vapor deposition of diamond films,” Phys. Rev. B, vol. 42, pp. 9458–9471, 1990.

[15] L. J. Karssemeijer and A. Fasolino, “Phonons of graphene and graphitic materials derived from the empirical potential lcbopii”. Surf.sc., vol. 605, no. 17-18, pp. 1611–1615, 2011.

[16] J. Maultzsch, S. Reich, C. Thomsen, H.requardt, and P. Ordej´on, “Phonon dispersion in graphite,” Phys. Rev. Lett, vol. 92, no. 7, p. 075501, 2004.

[17] M. Mohr, J. Mailtzsch, E. Dobardˇzi´c, S. Reich, I. Miloˇsevi´c, M. Damnjanovi´c, A. Bosak, M. krisch, and C. Thomsen, “Phonon dispersion of graphite by inelastic x-ray scattering.” Phys. Rev. B, vol. 76, no. 3, p. 035439, 2007.

[18] C. Oshima, T. Aizawa, R. Souda, Y. Ishizawa, and Y. Sumiyoshi, “Surface phonon dispersion curves of graphite (0001) over the entire energy region.” Solid State Commun., vol. 65, no. 12, pp. 1601–1604, 1988.

[19] S. Siebentritt, R. Pues, K. Rieder, and A. Shikin, “Surface phonon dispersion in graphite and in a lanthanum graphite intercalation compound,” Phys. Rev. B, vol. 55, no. 12, pp. 7927–7934, 1997.

[20] N. Mounet and N. Marzari, “First-principles determination of the structural, vibrational and thermodynamic properties of diamond, graphite, and derivatives”. Phys.Rev. B, vol. 71, no. 205214, 2005.

[21] K. Zakharchenko, M. I. Katsnelson, and A. Fasolino, “Finite temperature lattice properties of graphene beyond the quasiharmonic approximation,” Phys. Rev. Lett., vol. 102, no. 4, p. 046808, 2009.

[22] H. J. Monkhorst and J. D. Pack, “Special points for brillouin-zone

integrations,”Phys. Rev. B, vol. 13, no. 12, p. 51885192, 1976.

[23] T. H. K. Barron, J. G. Collins, and G. K. White, “Thermal-expansion of solids at low-temperatures,” Adv. Phys., vol. 29, no. 4, pp. 609–730, 1980.

[24] K. Zakharchenko, Temperature effects on graphene from a flat crystal to a 3D liquid. Ipskamp Drukkers, Enschede, 2011.

[25] C. Zener, Influence of Entropy on Phase Stabilization. Edited by P.S. Rudman, J.

Stringer and R.I. Jaffe, Phase Stability in Metals and Alloys, McGraw-Hill,New York , 1967.

[26] E. N. Koukaras, G. Kalosakas, C. Galiotis, and K. Papagelis. Phonon properties of graphene derived from molecular dynamics simulations. Scientific Reports,5, 2015.

[27] Luuk Coopmans "Temperature dependence of the phonons of graphene" Bachelor Thesis, 2016.

[28] Andry K. Geim and Allan H. MacDonald, "Graphene: Exploring Carbon Flatland", Physics Today, 60, pp. 35-40, (2007).

[29] N. M. Peres, "Graphene: New Physics in Two Dimensions", Europhysics News, 40/3, doi: 10.1051/epn/2009501, pp. 17-20, (2009).

[30] Mandar M. Deshmukh and Vibhor Singh, "Graphene- An Exciting

Two- Dimensional Material for Science and Technology", Resonance, 16, pp. 238-253, (2011).

[31] H. S. Philip Wong and Deji Akinwande, "Carbon Nanotube and Graphene Device Physics", Cambridge University Press, (2011).

[32] M. F. Craciun, S. Russo, M. Yamamoto and S. Tarucha"Tuneable Electronic Properties in Graphene", Nano Today, 6, pp. 42-60, 23 Jan (2011).

[33] Ji-Yong Park, "Carbon Nanotube Electronics", edited by Ali Javey and Jing Kong, Springer, pp. 1-42, (2009).

[34] Supriyo Datta, "Quantum Transport: Atom to Transistor", Cambridge University Press, (2005).

[35] Luke Anthony Kaiser Donev, "Carbon Nanotube Transistors: capacitance Measurements, localized damage, and uses as gold scaffolding", Cornell University, 3-34, (2009).

[36] Yanwu Zhu et al., "Graphene and Graphene Oxide: Synthesis, Properties, and Applications", Advanced Materials, 22, 3906-3924, (2010).